Studies on Diamond like Sn doped ZnO Nanostructures prepared via co-precipitation approach for improving photo-catalytic application

S. JAGADHESAN[a], V. SENTHILNATHAN[b], T. S. SENTHIL[c*]
[a]Department of Physics, Easa College of Engineering and Technology, Coimbatore-641105, India
[b]Department of Physics, Government Arts College, Udumalpet – 642126, India
[c]Department of Physics, Erode Sengunthar Engineering College, Thudupathi, Erode -638476, India

In this paper, pure Zinc Oxide (ZnO) nanoparticles (NPs) and Tin (Sn) doped ZnO nanostructures (NSs) prepared by using Co-precipitation approach are reported. The hexagonal wurtzite structure of pure ZnO and Sn (0.05% & 0.075%) doped ZnO NSs were analyzed by powder X-ray diffraction (PXRD) technique and the presence of various functional groups were identified by Fourier Transform Infrared Spectroscopy (FTIR) analysis. The optical energy gap was estimated by Tauc's plot under UV-Vis absorbance spectra. The shape and surface morphology of pure ZnO and diamond like structured Sn (0.075%) doped ZnO NSs are analysed by using FESEM and HR-TEM analysis. Sn (0.075%) doped ZnO NSs shows higher catalytic properties for the degradation of MB dye molecules under UV light, which provides promising application for detecting and eliminating organic pollutant.

1. Introduction

In recent decades, refractory organic pollutants can be degraded by using photo-catalysts of TiO_2 and ZnO wide-band gap semiconducting materials under UV irradiation [1]. Compared with TiO_2 nanoparticles, ZnO shows higher photo-catalytic efficiency in both acidic and basic medium for the degradation of organic dyes, which has been reported by various researchers [2–4]. In addition, ZnO material absorbs more light quanta than TiO_2 material [5, 6]. Zinc oxide (ZnO) has large exciton binding energy (60 mV) and shows various applications in many devices such as ultrasonic transducers, piezoelectric transducers, varistors, phosphors, pigments, photoelectric and UV-absorbers [7–13]. Nowadays, doping is a most powerful technique to improve the charge separation in the semiconductor systems, compared with various dopants Sb, Sn, Er and Al materials have been widely used [14, 15]. Among them, Sn is one of the most important doping element for improving the photo-catalytic activity of ZnO [16]. Because, doping of Sn with ZnO material shows the different structure of electronic shell and its the ionic radius of Sn^{4+} (0.69 Å) are similar to Zn^{2+} (0.74 Å) [17]. Sun et al. reported the effect of Sn doping in ZnO for the degradation of Methylene Blue (MB) dye solution under sunlight irradiation. They reported that the Sn doped ZnO nanoparticles greatly enhances the photo-catalytic activity compared with pure ZnO nanoparticles [1].

Various synthesis approaches have been used for the preparation of pure and doped ZnO nanomaterial, among them sol–gel processes [18], co-precipitation [19], aqueous solution deposition [20] and mechanochemical processing [21] are important. Compared with all other methods, co-precipitation method is one of the simplest and inexpensive method. By using this method the size and shape of the particles can be easily controlled by altering the pH of the medium [22]. The present study focused on diamond like structured Sn doped ZnO NSs prepared via co-precipitation approach for the photo-degradation of Methylene Blue (MB) dye. Nowadays most of the textile industries discharge MB dye as waste. The discharged dye is very harmful to human and it causes vomiting, heart rates, cyanosis, tissue necrosis, skin diseases and intestinal problems [22]. So in our study, we were choosing MB dye as a model pollutant for dye degradation process.

2. Materials and methods

2.1. Materials for synthesis of pure and Sn doped ZnO NSs

The Zinc sulfate Heptahydrate ($ZnSO_4 \cdot 7\ H_2O$), Sodium Hydrogen Carbonate ($NaHCO_3$) and Tin (II) chloride dihydrate ($SnCl_2.2H_2O$) chemicals were used for the synthesis of diamond like structured Sn doped ZnO nanostructures. Al the chemicals were purchased from Merck.

2.2. Synthesis of pure ZnO NPs

In each 200ml beaker, 0.1 M zinc sulfate heptahydrate ($ZnSO_4 \cdot 7H_2O$) and 0.1M sodium hydrogen carbonate

($NaHCO_3$) was taken with 100 ml double distilled (DD) water. After that 30ml of diluted sodium hydrogen carbonate solution was added slowly into the diluted solution of zinc sulfate heptahydrate under constant stirring at 30 min. After stirring process, the solution was washed with DD water and ethanol. Finally, the obtained solution turn around white color precipitate and the precipitate was dried in hot air oven at 150ºC for 1h. During this drying process, $Zn(OH)_2$ was fully changed into ZnO NPs. Finally, pure ZnO NPs was annealed at 450°C and used for further analysis.

2.3. Synthesis of diamond like Sn doped ZnO NSs

Firstly, 0.1M zinc sulfate heptahydrate was taken in 100 ml of DD water and then doping material of Tin (II) chloride dihydrate ($SnCl_2.2H_2O$) (0.02%, 0.04% & 0.06%) was slowly added into the diluted solution of zinc sulfate heptahydrate. Then, 30 ml sodium hydrogen carbonate was added slowly into the above mixed solution. After that the solutions were centrifuged and washed in a similar way as mentioned above. The obtained precipitate was dried at 150 ^{o}C for 1 h and annealed at 450°C. Finally, the obtained Sn doped ZnO NSs were used for further analysis.

2.4. Photocatalytic dye degradation studies

The photocatalytic performance was carried out by using 15 Watts UV lamp (Philips TUV-08). In the photo-catalytic application, pure and Sn (0.02 %, 0.04 % and 0.06 %) doped ZnO NSs has been investigated for MB organic dye degradation under UV light irradiation at room temperature. To investigate the photo-catalytic performance, 0.03 gm Sn (0.02 %, 0.04 % and 0.06 %) doped ZnO NSs samples were slowly dissolved in 30 ml of 100 μm aqueous solution of MB dye. To attain the adsorption/desorption equilibrium, the prepared sample was kept at dark condition. After that, the sample was irradiated under UV light source and the irradiated samples were taken at every 15 min time interval. After the filtration, the filtered samples were measured using UV-Vis absorption spectra. The maximum absorption for MB dye at λ= 663 nm was recorded in that spectra. The de-colorization efficiency of the synthesized materials was calculated by the following formula:

$$\text{De-colorization efficiency } (D_{eff}) = [C_0 - C_t / C_0] \times 100$$

where, C_0 and C_t represents the initial concentration of MB and the concentration of dye solution at different time interval.

2.5. Characterization Techniques

The power X-ray diffraction (PXRD) pattern shows the phase purity of synthesized material and it was identified by the instrument of Pro Penalty CAL with Cu-Kα radiation (1.5406 Å). FTIR analysis was carried

out by using the instrument of Perkin-Elmer spectrometer in the range between 4000-400 cm^{-1}. The optical analysis was carried out by the instrument of UV-Visible (JASCO V650) spectrometer. The FESEM analysis was recorded by using the instrument of JEOL JS-6390 combined with an EDAX spectrometer.

3. Result and discussion

3.1. Powder X-ray diffraction studies

The PXRD patterns of pure ZnO and Sn (0.05%, 0.075%) doped ZnO nanostructures are shown in Fig.1. All the diffraction peaks are corresponds to ZnO wurtzite structure of (100), (002), (101), (102), (110), (103), (200), (112) and (201) planes and all are well matched with standard JCPDS NO: 36-1451 [22, 23]. The intensity of doped ZnO peak decreases and it is due to the addition of Sn (0.05%, 0.075%) content. The reduction of intensity may attribute to the incorporation of Sn ions and which affects the density effects of native point defects such as vacancies, interstitials and antisite defects [24]. In addition, the higher intensity of pure ZnO (101) peak was shifted towards to the higher angle side due to the addition of Sn (0.05%, 0.075%) content which is shown in Fig.2. This shift may happen owing to the replacement of Zn^{2+} ions by Sn^{4+} ions in the ZnO lattice, due to the similarity of ionic radius of Zn^{2+} (0.74 Å) and Sn^{4+} (0.69 Å) [25].
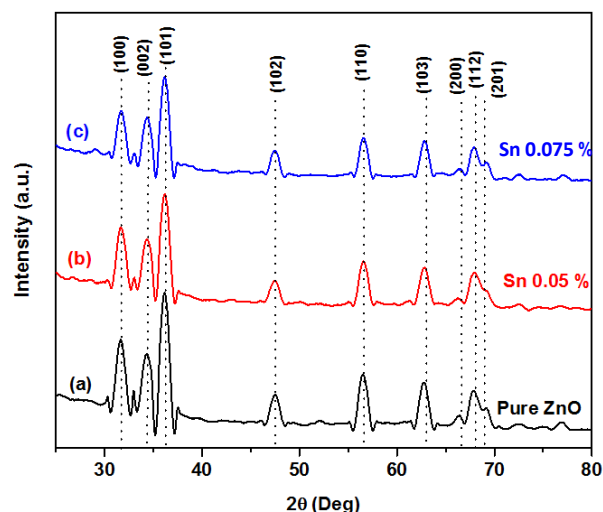

Fig. 1. Powder XRD Pattern of (a) Pure ZnO NPs and (b & c) different concentration of Sn (0.05% and 0.075%) doped ZnO NSs

The average crystallite size was calculated by using Scherrer's formula and the calculated values are found to 60, 65 and 70 nm for pure ZnO and Sn (0.05 % and 0.075 %) doped ZnO NSs respectively. The grain size linearly increases with the increase of dopant concentrations of Sn^{4+} and it is shown in Fig. 3.
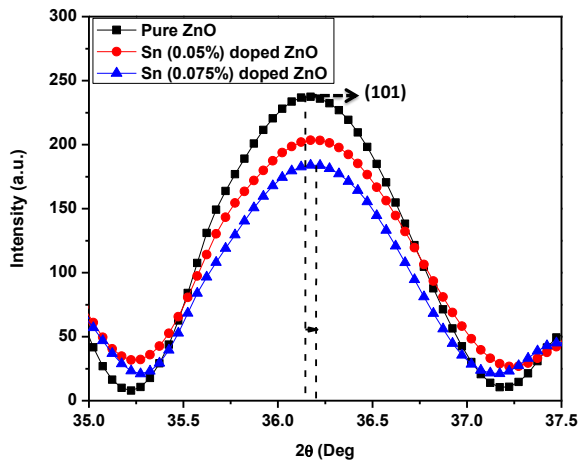
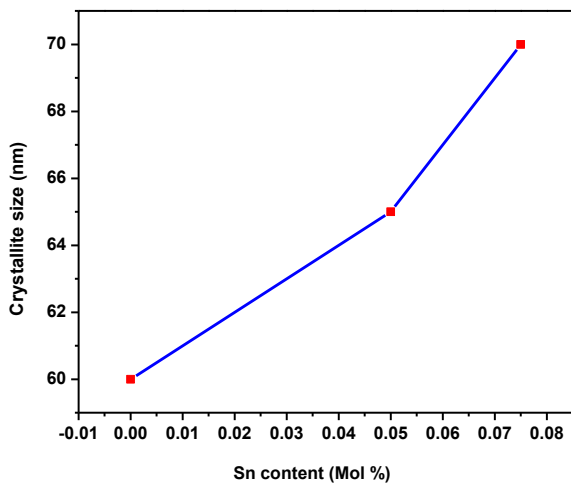*Fig. 2. Sn concentration dependent shift in (101) diffraction peak*

Fig. 3. Variation of crystallite size for pure and Sn doped ZnO samples

3.2. Fourier Transform Infrared (FT-IR) Spectroscopy

Fig. 4 reveals the FTIR spectrum of synthesized pure ZnO and Sn (0.075%) doped ZnO NSs. A small observed band at 2934 cm^{-1} is attributed to the CH_2 asymmetric stretching vibration [22]. The bands at 3304 cm^{-1} and 1633 cm^{-1} denotes H–O–H bending vibrations, possibly the presence of water (H_2O) content in the synthesized material [22]. The band at 2367 cm^{-1} is attributed to the presence of CO_2 molecule in the air medium [22]. The peak at 1125 cm^{-1} indicates the presence of sulphate group in the precursor material [22]. The small peaks observed at 474 cm^{-1} and 670 cm^{-1} indicates the bending vibration of Zn-O stretch and Sn–O stretch [26]. The Sn-O stretch occurs due to the replacement of Sn^{4+} ions by Zn^{2+} ions [26].
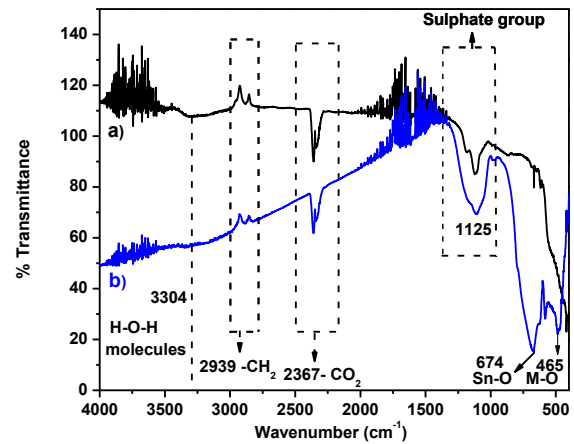

Fig. 4. FTIR spectrum of (a) Pure ZnO and (b) Sn (0.075%) doped ZnO NSs

3.3. UV-Visible Spectroscopy

Fig. 5 (a) reveals the UV-Visible absorption spectra of pure and Sn (0.05 % and 0.075 %) doped ZnO samples. The wavelength was observed at 305 nm, 307 nm and 311 nm respectively for pure ZnO and Sn (0.05 % and 0.075 %) doped ZnO samples.
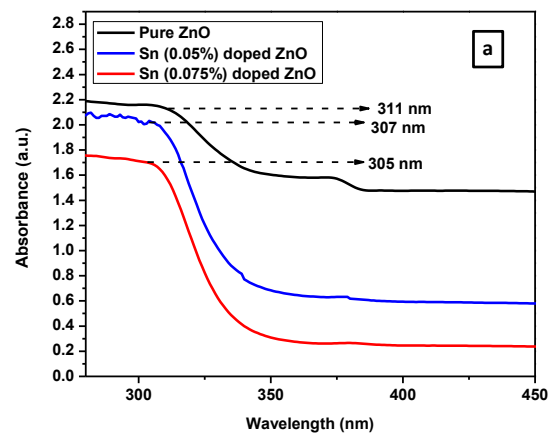

Fig. 5. (a) UV-Vis spectrum of pure ZnO & Sn doped (0.05% & 0.075%) ZnO NSs

The optical band gap of the prepared sample was calculated by using Tauc's relation [9]. The direct band gap of pure ZnO and Sn (0.05 % and 0.075 %) doped ZnO samples were plotted by using $(\alpha h\upsilon)^{1/2}$ vs $(h\upsilon)$ relation and is shown in Fig.5 (b). Where, α, h, υ and λ denotes the absorbance coefficient, planks constant, velocity of light and wave length of light. The direct band gap energy of pure ZnO and Sn (0.05 % and 0.075 %) doped ZnO was found to be 3.38 eV, 3.72eV and 3.79 eV respectively. From the observed optical band gap values, it should be noted that the band gap was slightly decreases with the addition of Sn concentration. This is due to Burstein-Moss effect, which means the doping creates degenerate energy levels with band-filling and that causes Fermi level to move above the conduction band edge [27]. The similar

result was reported by Chahmat et al. and they reported that the energy band gap decreases with increasing concentration of Sn (1 at.% to 5 at.%) [28].
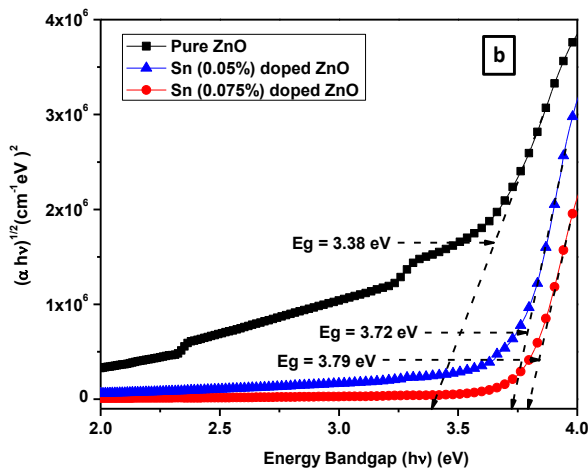

Fig. 5. (b) Band gap of pure ZnO & Sn doped (0.05% & 0.075%) ZnO NSs

3.4. Morphological studies

Fig. 6 (a & b) reveals the Field Emission Scanning Electron Microscopy (FESEM) spectrum of pure ZnO NSs and 6 (c) shows the diamond like structured Sn (0.05 % and 0.075 %) doped ZnO NSs. The prepared ZnO NSs are spherical in shape and well agglomerated, and it was correlated to the HR-TEM analysis. Fig. 6 (c) clearly shows that the Sn (0.05 % and 0.075 %) doped ZnO NSs are similar to diamond like structure and it was also confirmed by the HR-TEM analysis.
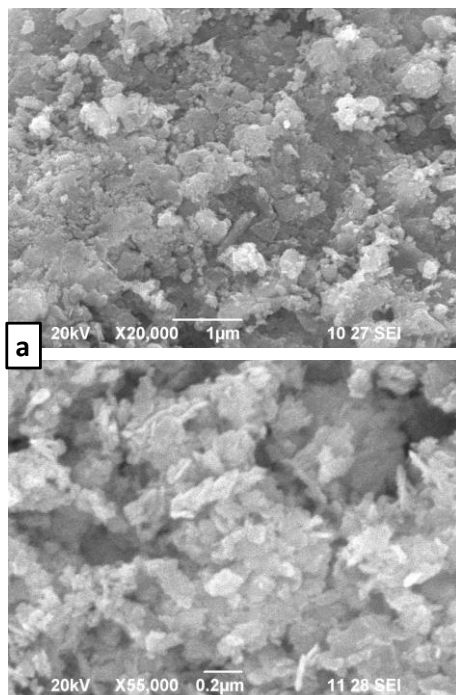

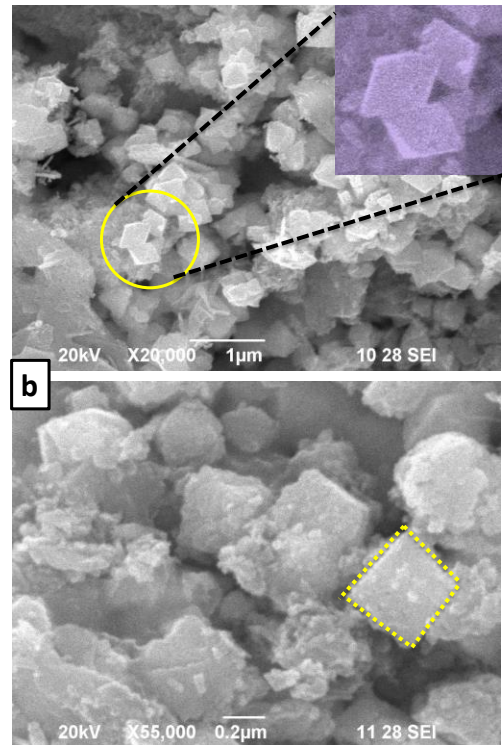*Fig. 6(a). Different magnification of FESEM analysis of pure ZnO NPs*

Fig. 6(b). Different magnification of FESEM analysis of diamond like Sn (0.05%) doped ZnO NSs
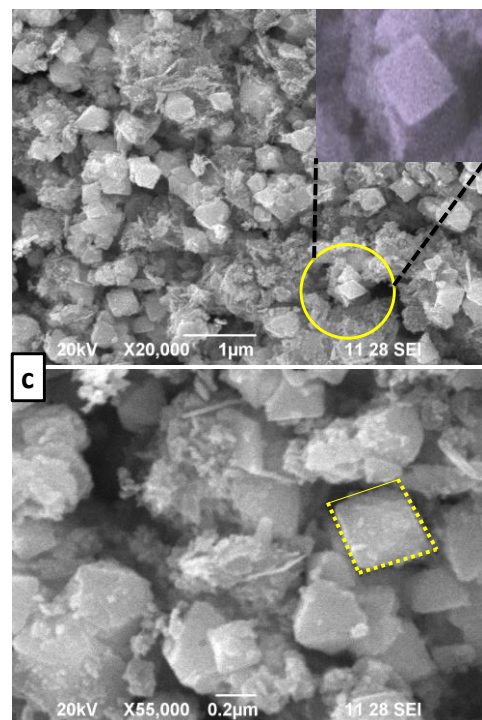

Fig. 6(c). Different magnification of FESEM analysis of diamond like Sb (0.075%) doped ZnO NSs

Fig.7 (a & b) shows the EDAX spectrum of pure ZnO NPs and Sn (0.075 %) doped ZnO NSs. From the figure, it should be noted that there is no impurities were present in the pure ZnO & Sn doped ZnO materials.
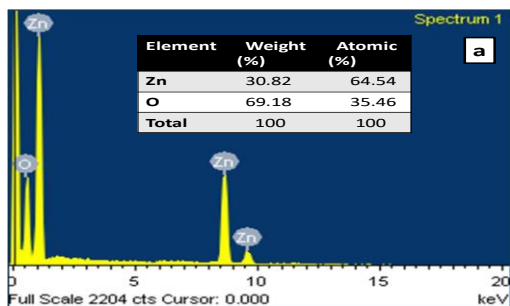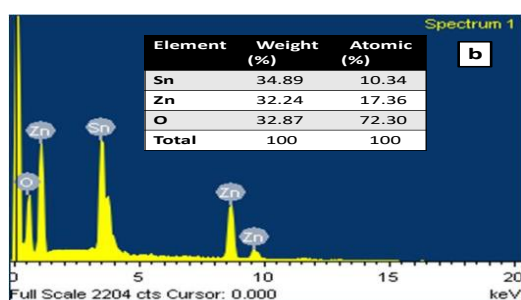
Fig. 7(a). EDAX analysis of pure ZnO NSs

Fig. 7(b). EDAX analysis of Sn (0.075%) doped ZnO NSs

The High Resolution Transmission Electron Microscopy (HRTEM) analysis was carried out using Tecnai G2-20 with an accelerating voltage of 200 KV. The HRTEM image of pure ZnO NPs and Sn (0.075%) doped ZnO NSs was shown in Fig. 8(a & b). The spherical ZnO NPs size was found to be 54 nm approximately. The uniform distribution of diamond like structure was confirmed from the Fig.8(b).
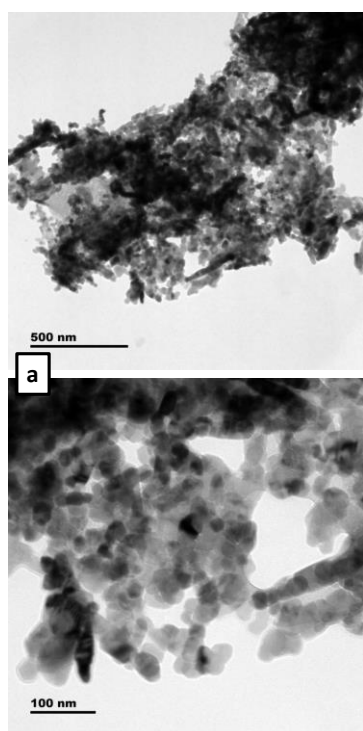

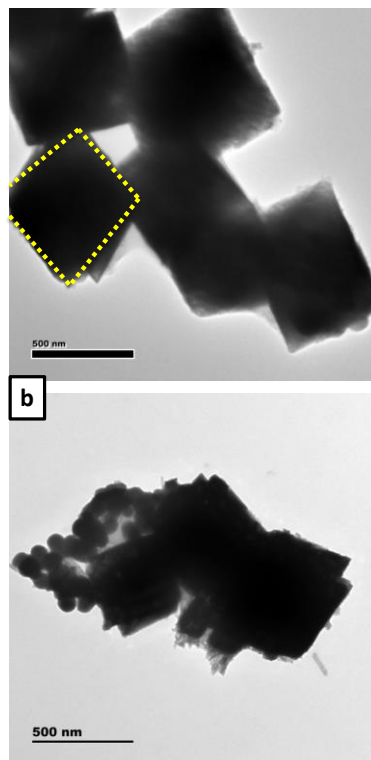Fig. 8(a). Different magnification of HRTEM image of pure ZnO NSs

Fig. 8(b). HRTEM image of diamond like Sn (0.075%) doped ZnO NSs

3.5. MB dye degradation studies

The photo-catalytic performance of as synthesized and Sn (0.05 % and 0.075 %) doped ZnO NSs was evaluated through MB dye under UV light. Fig. 9 (a, b & c) illustrates the MB dye degradation by using Sn (0.05 %) doped ZnO NSs and Fig. 9(d, e & f) represents the MB dye degradation by using Sn (0.075 %) doped ZnO NSs at different light irradiation time and different pH conditions. From the UV-Vis absorption spectra it should be noted that the characteristic absorption peak of MB (663 nm) dye decreases linearly with an increase of irradiation time. The Sn (0.075%) doped ZnO NSs degrades the MB dye completely within 2 hr than the Sn (0.05%) doped ZnO NSs.

Fig. 10 (a & b) shows the dye degradation efficiency of 0.05% and 0.075% Sn doped ZnO NSs. The Sn (0.075%) doped ZnO NSs exhibit higher photo-catalytic activity at pH=7 and its efficiency was observed as 92%. The enhanced photo-catalytic activity of Sn doped (0.075%) ZnO NSs is due to improved photo generated electron–hole pair separation, which leads to the enhanced dye adsorption [1]. In addition, the photo-catalytic activity of Sn doped ZnO NSs increases with increase of dopant concentration. The reason may be the enhanced singly ionized oxygen vacancies and defect concentrations [17]. In addition to this, the replacement of zinc ions by Sn ions also induces the performance. From these results we can say that the surface of Sn (0.075%) doped ZnO NSs played a vital role in the degradation of MB dye.
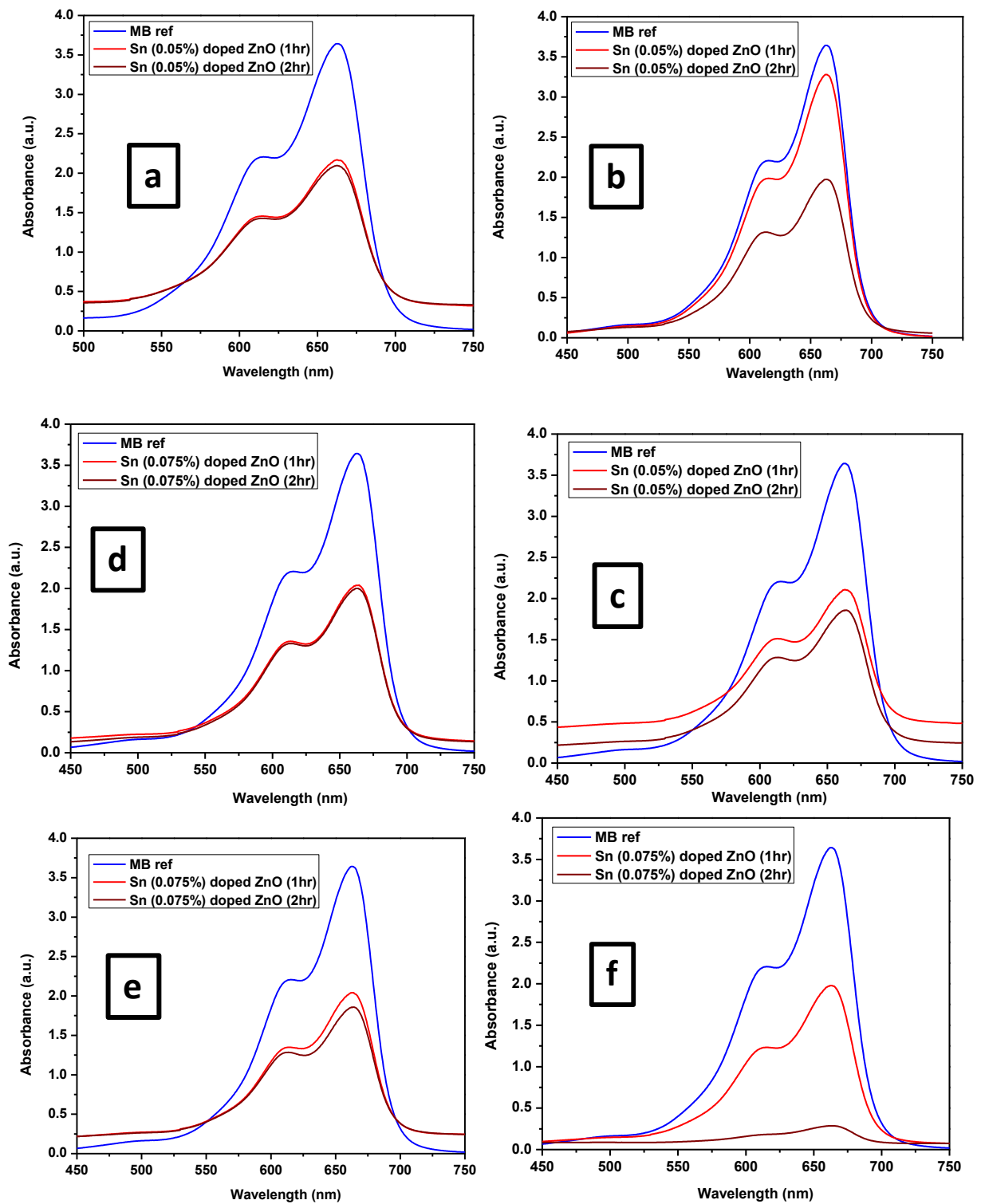
Fig. 9. The time dependent UV-Vis absorption spectra for MB removal (pH = 3, 5 & 7) of (a, b & c) 0.05% and (d, e & f) 0.075 mol% of Sn doped ZnO NSs
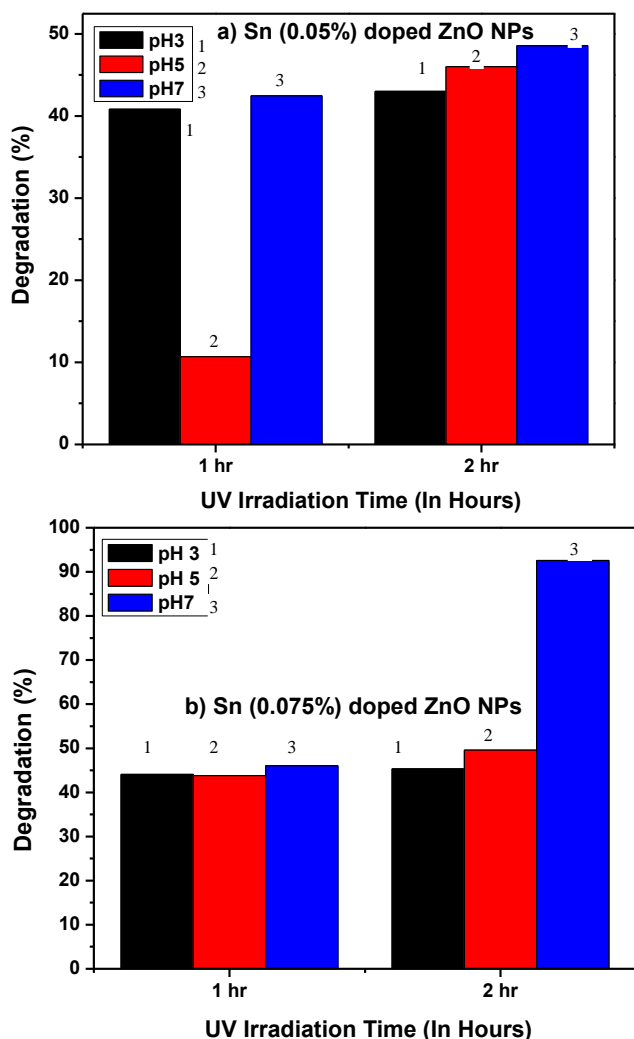
Fig. 10. (a & b) Dye degradation Efficiency graph for Sn (0.05% & 0.075%) doped ZnO NSs

4. Conclusion

A Co-precipitation approach of pure ZnO NPs and diamond like structured Sn (0.05% & 0.075%) doped ZnO NSs was reported in the present investigation. The structural and optical properties of synthesized materials were investigated. The optical band gap of pure ZnO NPs was linearly increases with Sn concentration. The diamond like structures of Sn (0.05% & 0.075%) doped ZnO NSs was clearly confirmed by using FESEM and HRTEM analysis. The synthesized Sn (0.075%) doped ZnO NSs were found to be effective photo-catalyst for the degradation of MB dye and it exhibits 92% degradation efficiency at 2 hr light irradiation. The enhanced photo-catalytic activity is due to the presence of more number of active sites presence in the prepared material. So, this study clearly demonstrated that diamond like structured Sn (0.075%) doped ZnO NSs is the promising candidate for the removal of MB dye for large scale applications.

Reference

[1] J. H. Sun, S. Y. Dong, J. L Feng, X. J. Yin, X. C. Zhao, Journal of Molecular Catalysis A: Chemical **335**, 145 (2011).
[2] M. Muruganandham, J. J. Wu, Appl. Catal. B: Environ **80**, 32 (2008).
[3] J. C. Lee, S. Park, H. J. Park, J. H. Lee, H. S. Kim, Y. J. Chung, J. Electroceram. **22**, 110 (2009).
[4] A. A. Khassin, T. M. Yurieva, V. V. Kaichev, V. I. Bukhtiyarov, A. A. Budneva, E. A. Paukshtis, V. N. Parmon, J. Mol. Catal. A **175**, 189 (2001).
[5] S. F. Chen, W. Zhao, W. Liu, S. J. Zhang, Appl. Surf. Sci. **255**, 2478 (2008).
[6] S. Rehman, R. Ullah, A. M. Butt, N. D. Gohar, J. Hazard. Mater. **170**, 560 (2009).
[7] N. Senthil Kumar, M. Ganapathy, S. Sharmila, M. Shankar, M. Vimalan, I. Vetha, J. Alloys and Compounds **703**, 624 (2017).
[8] N. K. Zayer, R. Greef, K. Rogers, A. J. C. Grellier, C. N. Pannell, Thin Solid Films **352**, 179 (1999)
[9] T. K. Gupta, J. Am. Ceram. Soc. **73,** 1817 (1990)
[10] C. Panatarani, I. W. Lenggoro, K. Okuyama, J. Phys. Chem. Solids **65**, 1843 (2004).
[11] Y. S. Wang, P. J. Thomas, P. O'Brien, J. Phys. Chem. B **110**, 4099 (2006).
[12] A. Petrellaa, P. D. Cozzolia, M. L. Currib, M. Striccolib, P. Cosmaa, A. Agostiana, Bioelectrochem. Bioenerg. **63**, 99 (2004).
[13] A. Becheri, M. Durr, P. L. Nostro, P. Baglioni, J. Nanopart. Res. **10**, 679 (2008).
[14] H. Benelmadjat, B. Boudine, O. Halimi, M. Sebais, Opt. Laser Technol, **41**, 630 (2009).
[15] J. Wang, Y. P. Xie, Z.H. Zhang, J. Li, X. Chen, L. Q. Zhang, R. Xu, X. D. Zhang, Sol. Energy Mater. Sol. C **93**, 355 (2009).
[16] Z. J. Yang, L. L. Lv, Y. L. Dai, Z. H. Xv, D. Qian, Appl. Surf. Sci. **256,** 2898 (2010).
[17] C. Wu, L. Shen, H. Yu, Q. Huang, Y. C. Zhang, Materials Research Bulletin **46,** 1107 (2011).
[18] M. Peiteado, Y. Iglesias, J. D. Frutos, J. F. Fernandez, A. C. Caballero, Bol. Soc. Esp. Ceram. **45,** 158 (2006).
[19] C. Wang, X. M. Wang, B. Q. Xua, J. C. Zhao, B. X. Mai, P. A. Peng, G. Y. Sheng, J. M. Fu, J. Photochem. Photobiol. A: Chem. **168,** 47 (2004).
[20] K. Govender, D. S. Boyle, P. O'Brien, D. Binks, D. West, D. Coleman, Adv. Mater. **14,** 1221 (2002).
[21] A. Dodd, A. McKinley, M. Saunders, T. Tsuzuki, Nanotechnology **17**, 692 (2006).

[22] R. Jeyachitra, V. Senthilnathan, T. S. Senthil, J Mater Sci: Mater Electron. **29**(2), 1189 (2018).

[23] N. Senthilkumar, E. Nandhakumar, P. Priya, D. Soni, M. Vimalan, I. Vetha Potheher, New J. Chem. **41**, 10347 (2017).

[24] F. J. Sheini, M. A. More, S.R. Jadkar, K. R. Patil, V. K. Pillai, D. S. Joag, J. Phys. Chem. C **114**, 3843 (2010).

[25] S. Luo, Y. Shen , Z. Wu, M. Cao, F. Gu, L. Wang, Materials Science in Semiconductor Processing **41,** 535 (2016).

[26] Yas Al-Hadeethi, Ahmad Umar, Saleh. H. Al-Heniti, Rajesh Kumar, S. H. Kim, Xixiang Zhang, Bahaaudin M. Raffah, z2D Sn-doped ZnO ultrathin nanosheet networks for enhanced acetone gas sensing application, Ceramics International (2016), DOI:10.1016/j.ceramint.2016.11.031.

[27] M. H. Mamat, M. Z. Sahdan, Z. Khusaimi, A. Z. Ahmed, S. Abdullah, and M. Rusop, Optical Materials **32,** 696 (2010).

[28] N. Chahmat, T. Souier, A. Mokri, M. Bououdina, M. S. Aida, M. Ghers, Journal of Alloys and Compounds **593,** 148 (2014).

[*]Corresponding author: tssenthi@gmail.com